

Gaussian formula and spherical aberrations of the static and moving curved mirrors from Fermat's principle

Sylvia H. Sutanto* and Paulus C. Tjiang†

*Theoretical and Computational Physics Group, Department of Physics,
Faculty of Mathematics and Natural Sciences, Parahyangan Catholic University, Bandung 40141 - INDONESIA*

The Gaussian formula and spherical aberrations of the static and moving curved mirrors are analyzed using the construction of optical path length (OPL) and the application of the Fermat's principle to the OPL. The geometrical figures generated by the rotation of conic sections about their symmetry axes are considered for the shapes of the mirrors. By comparing the results in static and moving cases, it is shown that the focal lengths of the moving mirrors change by the factor of $1 - \frac{v^2}{c^2}$, and the spherical aberrations turn out to be speed as well as vertical distance dependences.

PACS numbers: 02.30.Xx; 42.15.-i; 42.15.Fr; 42.79.Bh

Keywords: Static and moving curved mirrors; Gaussian formula; Fermat's principle; focal lengths; spherical aberrations.

I. INTRODUCTION

In every discussion of geometrical optics, the so-called Fermat's principle hardly misses its part. Most textbooks on either elementary physics or optics discuss the application of the Fermat's principle to derive the Snell's laws of reflection and refraction¹. However, none of these books discuss the application of the principle on the curved mirrors and lenses. To the best of our knowledge, the first and the only discussion of the application of Fermat's principle on curved mirrors and lenses, particularly those of the spherical shapes, was given by Lemons with his proposal of the time delay function². On the other hand, the discussion on the moving plane mirrors was recently brought by Gjurchinovski, both using Huygens construction³ and Fermat's principle⁴. The same discussion had been presented for the first time more than 100 years ago by Einstein through his famous work on the special theory of relativity⁵. However, to the best of our knowledge, no similar discussion on the moving curved mirrors has been found yet.

The purpose of this work is to give a rigorous analysis on the moving curved mirrors and compare the results to the static ones. Although the common shapes of mirrors used in practical applications are the spherical and parabolic shapes, we shall consider the shapes of curved mirrors generated by the rotation of the two dimensional conic sections about their symmetry axes, which is inspired by Watson⁶. The calculations are performed straightforwardly without any introduction of time delay function, since it may provide clearer interpretations on the results.

The paper is organized as follows : in Section II, we shall review the general mathematical form of the conic sections, which shall be used to shape the curved mirrors. In this case, we shall follow the discussions of conic section provided by Baker⁷ and Watson⁶. In Section III we shall discuss the application of Fermat's principle to obtain the Gaussian formula and the spherical aberration relations. Some cases of the mirror shapes discussed in Section II will be examined. The same discussion for the moving curved mirrors will be given in Section IV, with some analysis on the results compared to the static cases. The discussion concludes in Section V, with some remarks on the future work for the moving curved lenses.

II. GENERAL CURVED MIRROR : THE CONIC SECTIONS

Let us consider the curved mirrors whose shapes are the geometrical figures generated from the rotation of two dimensional conic sections about their symmetry axes. These shapes are well known in the constructions of astronomical instruments⁶. It is also worth to note that the discussion of conic sections is also useful for construction of mathematical models to predict the theoretical change of corneal asphericity within the optical zone after myopia treatment⁸, although it is beyond our scope of discussion.

The general mathematical description of the two dimensional conic sections^{6,7,8} is given by

$$(1 - e^2)l^2 + h^2 - 2Rl = 0, \quad (\text{II.1})$$

where l is the horizontal distance from the optical center of the mirror system, h is the vertical distance from the principal axis of the mirror system, e is the eccentricity of the conic section, and R is the apical radius of curvature (apex), given by

$$R = \left\{ \frac{\left[1 + \left(\frac{dl}{dh} \right)^2 \right]^{\frac{3}{2}}}{\left| \frac{d^2l}{dh^2} \right|} \right\}_{h=0} \quad (\text{II.2})$$

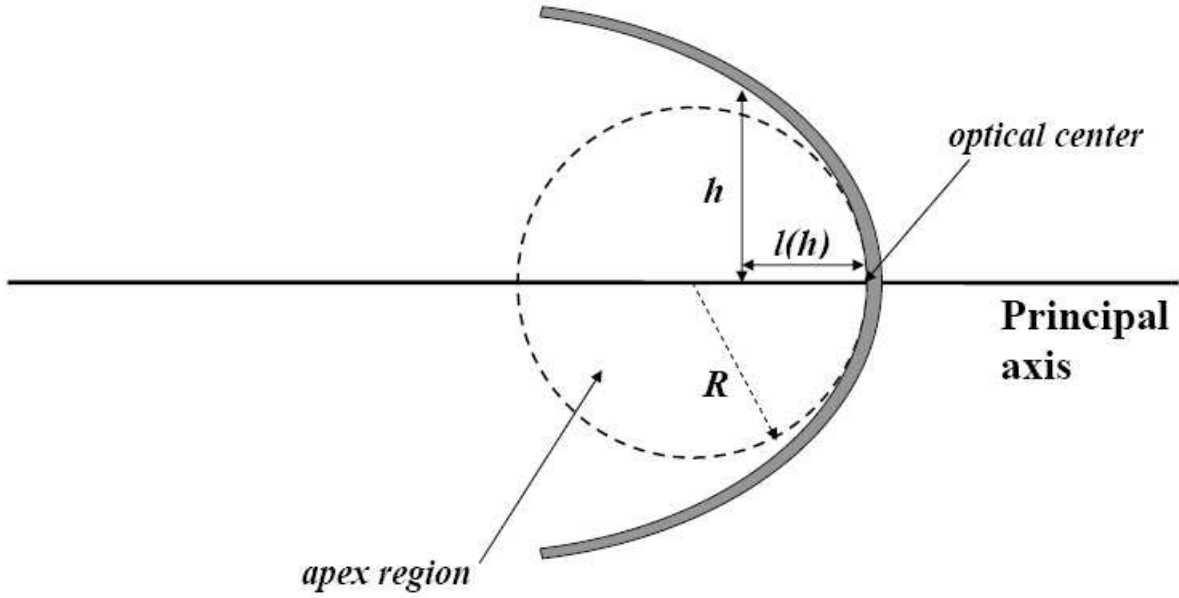


FIG. 1: The schematic diagram of a conic section. The area inside the dashed circle is the apex region of a conic section.

The apex region of a given conic section is illustrated by Figure 1.

Eq. (II.1) is known as *Baker's equation*^{7,8}. There are four types of mirror shapes based on the variation of eccentricity e :

1. $e = 0$ gives the equation of circle with radius R . Solving Eq. (II.1) for l with this type of conic section, we get

$$l_{\pm}(h) = \pm \left(R - \sqrt{R^2 - h^2} \right). \quad (\text{II.3})$$

2. $0 < e < 1$ gives the equation of ellipse with apical radius R . Solving Eq. (II.1) for l with this type of conic section, we get

$$l_{\pm}(h) = \pm \left(\frac{R - \sqrt{R^2 - (1 - e^2)h^2}}{1 - e^2} \right). \quad (\text{II.4})$$

3. $e = 1$ gives the equation of parabola with apical radius R . Solving Eq. (II.1) for l with this type of conic section, we get

$$l_{\pm}(h) = \pm \left(\frac{h^2}{2R} \right). \quad (\text{II.5})$$

4. $e > 1$ gives the equation of hyperbola with apical radius R . Solving Eq. (II.1) for l with this type of conic section, we get

$$l_{\pm}(h) = \pm \left(\frac{\sqrt{R^2 + (e^2 - 1)h^2} - R}{e^2 - 1} \right). \quad (\text{II.6})$$

The \pm signs in Eqs. (II.3) - (II.6) indicate concave / convex mirror systems. It is clear that the horizontal distance $l(h)$ is an even function of the vertical distance h , with $l(0) = 0$ according to the fact that the $l(h)$ vanishes at the optical center.

III. APPLICATIONS OF THE FERMAT'S PRINCIPLE ON THE STATIC CURVED MIRRORS

Figure 2 shows the propagation of light from point **A** to point **B**, with reflection of light at point **C** on the surface of the mirror.

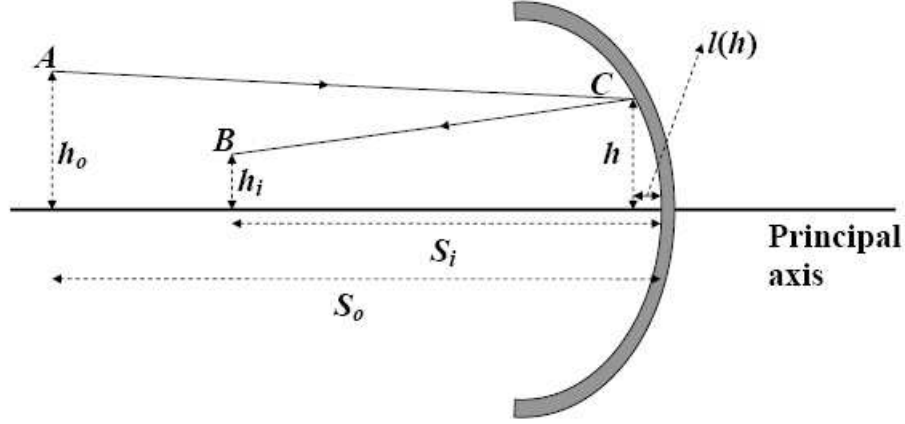


FIG. 2: The schematic diagram of the static curved mirror system. The (S_0, h_0) and (S_i, h_i) are sets of coordinates related to the object and its associated image, respectively. The solid line **A-C-B** is the optical path length (OPL) of the light.

The *optical path length* (OPL) of the light from **A** to **B** is

$$\text{OPL}(h) = S_0 \sqrt{\left[1 - \frac{l(h)}{S_0}\right]^2 + \left[\frac{h - h_0}{S_0}\right]^2} + S_i \sqrt{\left[1 - \frac{l(h)}{S_i}\right]^2 + \left[\frac{h_i - h}{S_i}\right]^2}. \quad (\text{III.7})$$

The traveling time of light can be obtain by dividing the OPL (III.7) with the speed of light c of the corresponding medium :

$$t(h) = \frac{S_0}{c} \sqrt{\left[1 - \frac{l(h)}{S_0}\right]^2 + \left[\frac{h - h_0}{S_0}\right]^2} + \frac{S_i}{c} \sqrt{\left[1 - \frac{l(h)}{S_i}\right]^2 + \left[\frac{h_i - h}{S_i}\right]^2}. \quad (\text{III.8})$$

The application of Fermat's principle can be accomplished by vanishing the first derivative of Eq. (III.8). The result is

$$\frac{dt}{dh}(h) = \frac{\frac{h-h_0}{S_0} - \left(1 - \frac{l(h)}{S_0}\right) \frac{dl}{dh}}{\sqrt{\left[1 - \frac{l(h)}{S_0}\right]^2 + \left[\frac{h-h_0}{S_0}\right]^2}} - \frac{\frac{h_i-h}{S_i} + \left(1 - \frac{l(h)}{S_i}\right) \frac{dl}{dh}}{\sqrt{\left[1 - \frac{l(h)}{S_i}\right]^2 + \left[\frac{h_i-h}{S_i}\right]^2}} = 0. \quad (\text{III.9})$$

Since it is very difficult to solve Eq. (III.9) for h , we shall analyze it by taking Taylor expansion of Eq. (III.9) near $h = 0$:

$$\frac{dt}{dh}(h) = \sum_{n=1}^{\infty} \frac{1}{(n-1)!} \frac{d^{n-1}t}{dh^{n-1}}(0) h^{n-1} = 0. \quad (\text{III.10})$$

which leads to

$$\frac{d^n t}{dh^n}(0) = 0, \quad n = 1, 2, 3, \dots \quad (\text{III.11})$$

A. The Gaussian formula of the static mirrors

The first two terms of Eq. (III.11) after the insertion of Eq. (III.8) lead to

$$\frac{\left(1 - \frac{l(0)}{S_0}\right) \dot{l}(0) + \frac{h_0}{S_0}}{\sqrt{\left(1 - \frac{l(0)}{S_0}\right)^2 + \frac{h_0^2}{S_0^2}}} + \frac{\left(1 - \frac{l(0)}{S_i}\right) \dot{l}(0) + \frac{h_i}{S_i}}{\sqrt{\left(1 - \frac{l(0)}{S_i}\right)^2 + \frac{h_i^2}{S_i^2}}} = 0, \quad (\text{III.12})$$

$$\begin{aligned} & \frac{\frac{1}{S_0} \left(1 + \dot{l}^2(0)\right) - \left(1 - \frac{l(0)}{S_0}\right) \ddot{l}(0)}{\sqrt{\left(1 - \frac{l(0)}{S_0}\right)^2 + \frac{h_0^2}{S_0^2}}} - \frac{\frac{1}{S_0} \left(\left(1 - \frac{l(0)}{S_0}\right) \dot{l}(0) + \frac{h_0}{S_0}\right)^2}{\left(\left(1 - \frac{l(0)}{S_0}\right)^2 + \frac{h_0^2}{S_0^2}\right)^{\frac{3}{2}}} \\ & + \frac{\frac{1}{S_i} \left(1 + \dot{l}^2(0)\right) - \left(1 - \frac{l(0)}{S_i}\right) \ddot{l}(0)}{\sqrt{\left(1 - \frac{l(0)}{S_i}\right)^2 + \frac{h_i^2}{S_i^2}}} - \frac{\frac{1}{S_i} \left(\left(1 - \frac{l(0)}{S_i}\right) \dot{l}(0) + \frac{h_i}{S_i}\right)^2}{\left(\left(1 - \frac{l(0)}{S_i}\right)^2 + \frac{h_i^2}{S_i^2}\right)^{\frac{3}{2}}} = 0, \end{aligned} \quad (\text{III.13})$$

where $\dot{l}(h)$ and $\ddot{l}(h)$ are the first and the second derivatives of $l(h)$ with respect to h , respectively.

In order to get a clear interpretation on these terms, we consider two assumptions which is generally made in geometrical optics :

- It is common to use the so-called *paraxial ray approximation*, i.e. when the rays intersect the principal axis at small angles. The consequences of the approximation are

$$\left| \frac{h_0}{S_0} \right| \ll 1, \quad \left| \frac{h_i}{S_i} \right| \ll 1, \quad (\text{III.14})$$

i.e. we may neglect the higher order contributions of $\frac{h_0}{S_0}$ and $\frac{h_i}{S_i}$ on Eq. (III.11).

- It is customary to consider mirrors whose curvatures are symmetric with respect to their associated principal axes. Consequently, the function $l(h)$ must be an even function : $l(-h) = l(h)$, and all odd derivatives of $l(h)$ vanish at $h = 0^2$. The shapes of mirrors discussed in Section II satisfy this condition.

Based on the assumptions above, Eqs. (III.12) and (III.13) lead to

$$\frac{h_0}{S_0} + \frac{h_i}{S_i} = 0 \quad \Longleftrightarrow \quad \frac{h_i}{h_0} = -\frac{S_i}{S_0}, \quad (\text{III.15})$$

$$\frac{1}{S_0} + \frac{1}{S_i} = 2\ddot{l}(0). \quad (\text{III.16})$$

Eq. (III.15) expresses the usual lateral magnification formula, and Eq. (III.16) is the Gaussian formula relating object distance S_0 and image distance S_i , with the focal length f defined as

$$f \equiv \frac{1}{2\ddot{l}(0)}. \quad (\text{III.17})$$

Applying Eq. (III.17) to each mirror shape given by Eqs. (II.3) - (II.6), it is interesting to note that the second derivative $\ddot{l}(0) = \frac{1}{R}$ regardless of the eccentricity e . Hence the focal length for any shape of mirror generated from a conic section is

$$f_{\pm} = \pm \frac{R}{2}. \quad (\text{III.18})$$

If the conic section is a circle, Eq. (III.18) gives the usual focal length of a spherical mirror, since the apex of a circle is equal to its radius. In general, Eq. (III.18) is equally true for any shape of mirror (generated by a conic section, where R is generalized to the apex of the associated conic section.

B. Spherical aberrations in the static mirrors

Spherical aberration occurs in the curved mirror system when the reflected light rays coming from the outer region of the mirror do not arrive to the same focal point as those from paraxial region⁹. The schematic diagram of the phenomenon is shown in Figure 3.

At the paraxial region, the Gaussian formula (III.16) holds. We may obtain the focal length of the curved mirror by setting $S_0 \rightarrow \infty$, i.e. when light source is relatively far away from the mirror, and the distance of the associated image S_i is equal to the focal length. By Eq. (III.15), the image height $h_i = 0$ regardless of the object height h_0 . As we consider light rays coming from

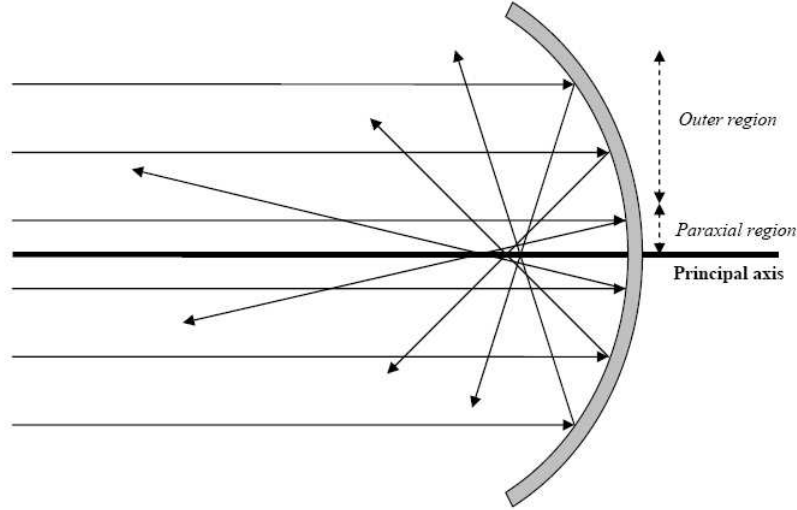


FIG. 3: The schematic diagram of the spherical aberration.

the outer region, we have to start from Eq. (III.9), take $S_0 \rightarrow \infty$ and $h_i = 0$, and solve the resulting equation for S_i . The result is

$$S_i(h) = f(h) = l(h) + \frac{h(1 - i^2(h))}{2i(h)}. \quad (\text{III.19})$$

It is clear from Eq. (III.19) that the intersections of the reflected rays to the principal axis depend on the vertical distance h in general.

Now we may analyze some examples of the curved mirrors discussed in Section II :

- **Spherical mirrors.** Inserting Eq. (II.3) into Eq. (III.19), we get

$$f(h) = \pm \left(R - \frac{R^2}{2\sqrt{R^2 - h^2}} \right) \quad (\text{III.20})$$

Figure 4 (for $e = 0$) shows the behavior of spherical aberration caused by a spherical concave mirror.

Eq. (III.20) indicates that the intersections of the reflected rays (or the extension of the reflected rays for the case of convex mirror) to the principal axis are coming closer to the optical center of the mirror as the vertical distance h increases. At the paraxial region where h is considerably small, Eq. (III.20) gives Eq. (III.18). At $h = \frac{\sqrt{3}}{2}R$, the reflected ray hits the optical center. At $\frac{\sqrt{3}}{2}R < h < R$, the intersection points between the extension of reflected rays and the principal axis in both concave and convex cases are getting farther from the optical center in the opposite directions. From Figure 4 (for $e = 0$), we may observed that Eq. (III.20) has asymptotic behavior at $h = R$.

- **Elliptic mirrors.** Inserting Eq. (II.4) into Eq. (III.19), we get

$$f(h, e) = \pm \left(\frac{R - \sqrt{R^2 - (1 - e^2)h^2}}{1 - e^2} + \frac{R^2 - (2 - e^2)h^2}{2\sqrt{R^2 - (1 - e^2)h^2}} \right) \quad (\text{III.21})$$

Figure 4 (for $0 < e < 1$) shows the behavior of spherical aberrations caused by elliptic concave mirrors.

Eq. (III.21) indicates that the spherical aberration of the elliptic mirror depends on both the vertical distance h and the eccentricity e . To look deeply into the equation, we expand Eq. (III.21) in terms of Taylor series at paraxial region up to the sixth order. The result is

$$f(h, e) = \pm \left(\frac{R}{2} - \frac{(1 - e^2)h^2}{4R} - \frac{(1 - e^2)(3 - e^2)h^4}{16R^3} - \frac{(5 - e^2)(1 - e^2)^2h^6}{32R^5} + O(7) \right) \quad (\text{III.22})$$

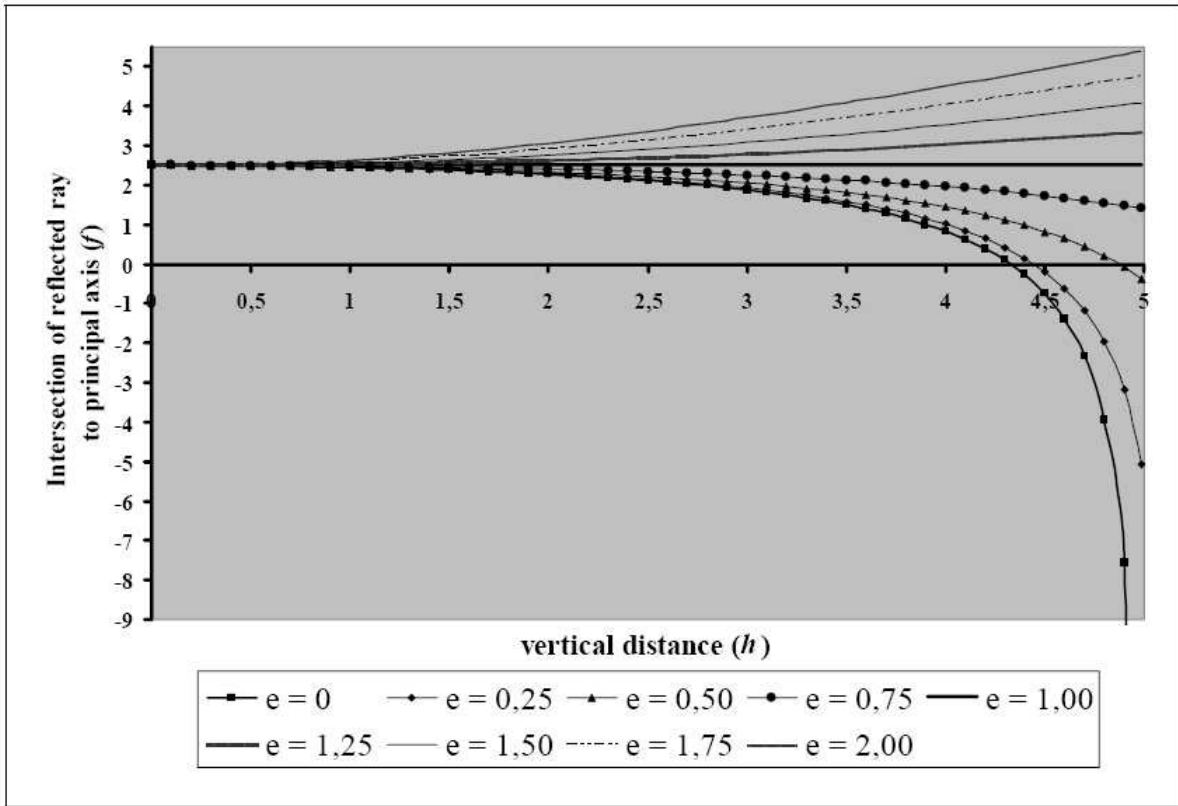


FIG. 4: Spherical aberration for concave mirrors of various conic sections. The plot with $e = 0$ shows the aberration of spherical mirror. The straight line shows the plot for parabolic mirror ($e = 1$).

Since $0 < e < 1$, Eq. (III.22) indicates clearly that the intersections of the reflected rays (or the extension of the reflected rays for the case of convex mirror) to the principal axis are coming closer to the optical center as the vertical distance h increases. At the paraxial region, again Eq. (III.21) leads to Eq. (III.18). Eq. (III.22) gives the same result as obtained by Watson using different approach⁶. From Figure 4 (for $0 < e < 1$), we may observed that Eq. (III.21) has asymptotic behavior at $h > R$ for a given e , which increases as e increases.

- **Parabolic mirrors.** Inserting Eq. (II.5) into Eq. (III.19), we get

$$f(h) = \pm \frac{R}{2}, \quad (\text{III.23})$$

i.e. the focal length given by Eq. (III.18). This indicates that the parabolic mirror does not suffer spherical aberration, as all the incoming light rays will intersect with the principal axis at the same point given by (III.23). There are many applications made possible by this kind of mirror, e.g. production of a beam of parallel rays from a single light source placed at the mirror's focal point.

- **Hyperbolic mirrors.** Inserting Eq. (II.6) into Eq. (III.19), we get

$$f(h, e) = \pm \left(\frac{\sqrt{R^2 + (e^2 - 1)h^2} - R}{e^2 - 1} + \frac{R^2 + (e^2 - 2)h^2}{2\sqrt{R^2 + (e^2 - 1)h^2}} \right) \quad (\text{III.24})$$

Figure 4 (for $e > 1$) shows the behavior of spherical aberrations caused by hyperbolic concave mirrors.

Like the elliptic mirror, Eq. (III.24) indicates that the spherical aberration of the hyperbolic mirror depends on both the vertical distance h and the eccentricity e . Comparing Eq. (III.24) with Eq. (III.21), it is clear that the hyperbolic and elliptic mirrors assume the same functional forms of $f(h, e)$. Again, we expand Eq. (III.21) in terms of Taylor series at paraxial region up to the sixth order. The result is

$$f(h, e) = \pm \left(\frac{R}{2} + \frac{(e^2 - 1)h^2}{4R} - \frac{(e^2 - 1)(e^2 - 3)h^4}{16R^3} + \frac{(e^2 - 5)(e^2 - 1)^2h^6}{32R^5} + O(7) \right) \quad (\text{III.25})$$

Eq. (III.25) indicates clearly that the intersections of the reflected rays (or the extension of the reflected rays for the case of convex mirror) to the principal axis are moving away from the optical center as the vertical distance h increases. At the paraxial region, Eq. (III.24) leads again Eq. (III.18). From Figure 4 (for $e > 1$), it is clear that no asymptotic behavior is observed.

IV. APPLICATIONS OF THE FERMAT'S PRINCIPLE ON THE MOVING CURVED MIRRORS

Now let us consider a mirror system which is moving parallel to the principal axis at a constant speed v relative to a rest observer. As shown in Figure 5, the mirror system is moving to the right. The light ray travels from point **A**, is reflected at point **C** on the surface of the mirror, and finally reaches point **B**. During the movement of the mirror system, it is important to keep in mind that the speed of light *remains the same*, as stated by the second postulate of the special theory of relativity⁵.

The OPL of the light from **A** to **C** is

$$l_a(h) = S_0 \sqrt{\left[1 + \frac{vt_a - l(h)}{S_0}\right]^2 + \left[\frac{h - h_0}{S_0}\right]^2}, \quad (\text{IV.26})$$

and the OPL from **C** to **B** is

$$l_b(h) = S_i \sqrt{\left[1 - \frac{vt_a + l(h)}{S_i}\right]^2 + \left[\frac{h_i - h}{S_i}\right]^2}. \quad (\text{IV.27})$$

The traveling time from **A** to **C** can be obtain from Eq. (IV.26) by dividing it with the speed of light c and solving the resulting equation for t_a . The result is

$$t_a(h) = \frac{S_0}{c} \gamma^2 \left[\sqrt{\left(1 - \frac{l(h)}{S_0}\right)^2 + \frac{1}{\gamma^2} \left(\frac{h - h_0}{S_0}\right)^2} + \beta \left(1 - \frac{l(h)}{S_0}\right) \right], \quad (\text{IV.28})$$

where $\beta \equiv \frac{v}{c}$ and $\gamma \equiv \left(1 - \frac{v^2}{c^2}\right)^{-\frac{1}{2}}$. Similarly, the traveling time from **C** to **B** can be obtain from Eq. (IV.26), which leads to

$$t_b(h) = \frac{S_i}{c} \gamma^2 \left[\sqrt{\left(1 - \frac{l(h)}{S_i}\right)^2 + \frac{1}{\gamma^2} \left(\frac{h_i - h}{S_i}\right)^2} - \beta \left(1 - \frac{l(h)}{S_i}\right) \right]. \quad (\text{IV.29})$$

The total traveling time is then $t(h) = t_a(h) + t_b(h)$.

Applying the Fermat's principle by vanishing the first derivative of the total traveling time $t(h)$, we obtain

$$\frac{\frac{h-h_0}{\gamma^2 S_0} - \left(1 - \frac{l(h)}{S_0}\right) \dot{l}(h)}{\sqrt{\left(1 - \frac{l(h)}{S_0}\right)^2 + \frac{1}{\gamma^2} \left(\frac{h-h_0}{S_0}\right)^2}} - \frac{\frac{h_i-h}{\gamma^2 S_i} + \left(1 - \frac{l(h)}{S_i}\right) \dot{l}(h)}{\sqrt{\left(1 - \frac{l(h)}{S_i}\right)^2 + \frac{1}{\gamma^2} \left(\frac{h_i-h}{S_i}\right)^2}} = 0. \quad (\text{IV.30})$$

For $v \ll c$, Eq. (IV.30) gives Eq. (III.9). As in the static case, Eq. (IV.30) is very difficult to solve for h , and we shall use the Taylor expansion (III.10) and the relation (III.11) to analyze it properly.

A. The Gaussian formula of the moving mirrors

The first two terms of the relation (III.11) obtained from Eq. (IV.30) give

$$\frac{\frac{h_0}{\gamma^2 S_0} - \left(1 - \frac{l(0)}{S_0}\right) \dot{l}(0)}{\sqrt{\left(1 - \frac{l(0)}{S_0}\right)^2 + \frac{1}{\gamma^2} \left(\frac{h_0}{S_0}\right)^2}} + \frac{\frac{h_i}{\gamma^2 S_i} + \left(1 - \frac{l(0)}{S_i}\right) \dot{l}(0)}{\sqrt{\left(1 - \frac{l(0)}{S_i}\right)^2 + \frac{1}{\gamma^2} \left(\frac{h_i}{S_i}\right)^2}} = 0, \quad (\text{IV.31})$$

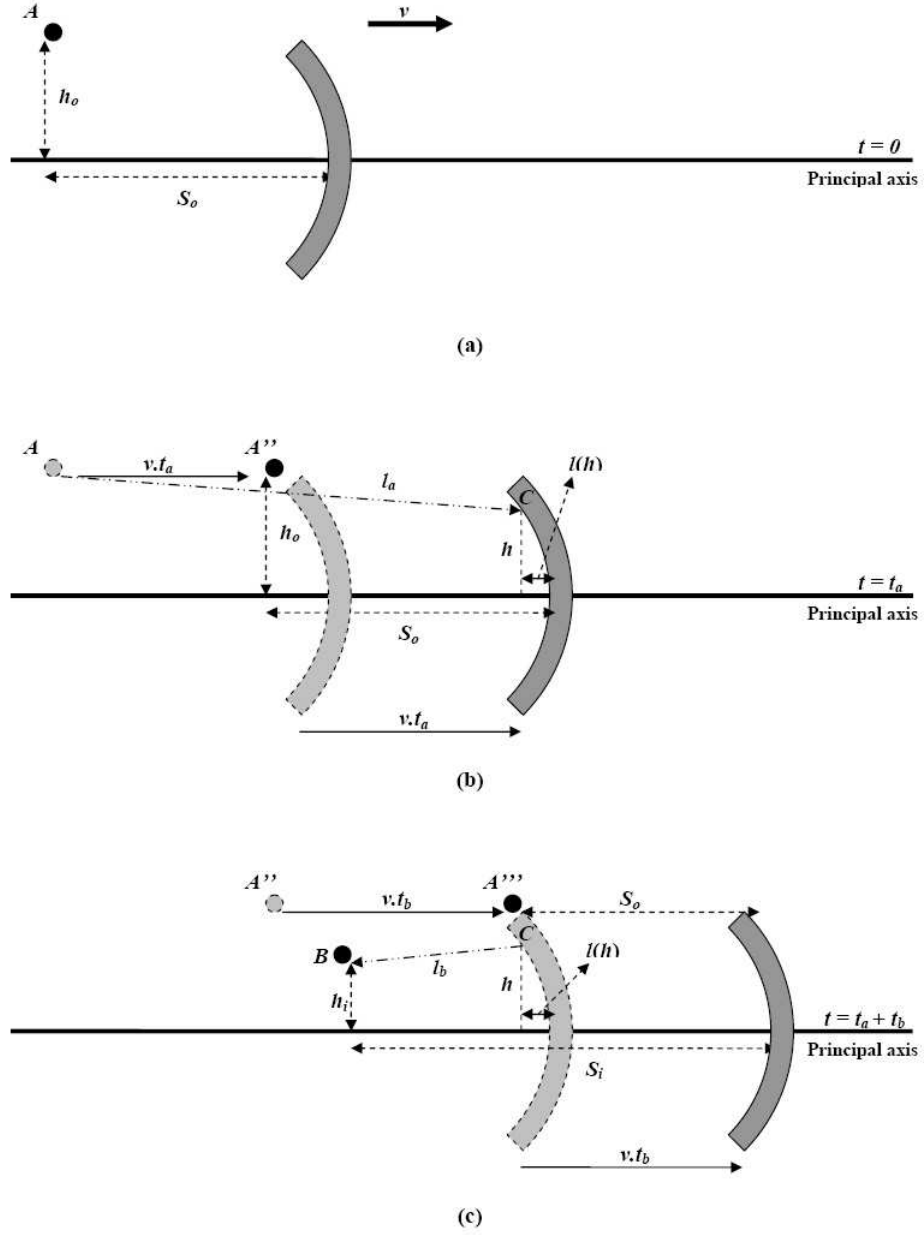


FIG. 5: The schematic diagram of the moving curved mirror system. The figures (a), (b) and (c) are arranged in chronological order. The OPL from **A** to **B** is shown by the dashed-double dotted line. During the movement of the system, the initial point is moving from **A** to **A'''**, so the distance between the initial point and the mirror is held constant at all time.

$$\begin{aligned}
 & \frac{\frac{1}{S_0} \left(\frac{1}{\gamma^2} + \dot{l}^2(0) \right) - \left(1 - \frac{l(0)}{S_0} \right) \ddot{l}(0)}{\sqrt{\left(1 - \frac{l(0)}{S_0} \right)^2 + \frac{h_0^2}{\gamma^2 S_0^2}}} - \frac{\frac{1}{S_0} \left(\left(1 - \frac{l(0)}{S_0} \right) \dot{l}(0) + \frac{h_0}{\gamma^2 S_0} \right)^2}{\left(\left(1 - \frac{l(0)}{S_0} \right)^2 + \frac{h_0^2}{\gamma^2 S_0^2} \right)^{\frac{3}{2}}} \\
 & + \frac{\frac{1}{S_i} \left(\frac{1}{\gamma^2} + \dot{l}^2(0) \right) - \left(1 - \frac{l(0)}{S_i} \right) \ddot{l}(0)}{\sqrt{\left(1 - \frac{l(0)}{S_i} \right)^2 + \frac{h_i^2}{\gamma^2 S_i^2}}} - \frac{\frac{1}{S_i} \left(\left(1 - \frac{l(0)}{S_i} \right) \dot{l}(0) + \frac{h_i}{\gamma^2 S_i} \right)^2}{\left(\left(1 - \frac{l(0)}{S_i} \right)^2 + \frac{h_i^2}{\gamma^2 S_i^2} \right)^{\frac{3}{2}}} = 0.
 \end{aligned} \tag{IV.32}$$

Considering that $l(h)$ is an even function and using the paraxial ray approximation (III.14), Eqs (IV.31) and (IV.32) lead to

$$\frac{1}{\gamma^2} \left(\frac{h_0}{S_0} + \frac{h_i}{S_i} \right) = 0 \quad \Longleftrightarrow \quad \frac{h_i}{h_0} = -\frac{S_i}{S_0}, \quad (\text{IV.33})$$

$$\frac{1}{S_0} + \frac{1}{S_i} = 2\gamma^2 \ddot{l}(0). \quad (\text{IV.34})$$

Comparing Eqs. (III.15) and (IV.33), it is clear that the lateral magnification formula is preserved, i.e. the magnification rule appears the same in either static or moving cases. The Gaussian formula, however, suffers a modification on the focal length of the mirror, i.e.

$$f \equiv \frac{1}{2\ddot{l}(0)} \implies \bar{f}(v) \equiv \frac{1}{2\gamma^2 \ddot{l}(0)} = \left(1 - \frac{v^2}{c^2} \right) f, \quad (\text{IV.35})$$

based on comparison between Eqs. (III.16) and (IV.34). The focal length is becoming shorter by the factor of $1 - \frac{v^2}{c^2}$. Inserting Eq. (III.18) into Eq. (IV.35), we obtain the focal length of moving curved mirror with the shape of a conic section as

$$\bar{f}(v) = \pm \left(1 - \frac{v^2}{c^2} \right) \frac{R}{2}. \quad (\text{IV.36})$$

B. Spherical aberrations in the moving mirrors

Using the same arguments similar to those used in the discussion of spherical aberration in Section III B, we shall start from Eq. (IV.30), take $S_0 \rightarrow \infty$ and $h_i = 0$, and solve the resulting equation for S_i . The result is

$$S_i(h) = f(h, v) = l(h) + \frac{h \left(\frac{1}{\gamma^2} - \dot{l}^2(h) \right)}{2\dot{l}(h)}. \quad (\text{IV.37})$$

Eq. (IV.37) differs from Eq. (III.19) by the factor $\frac{1}{\gamma^2}$ on the second term. Eq. (IV.37) indicates that the speed of the mirror contributes significantly to the spherical aberration together with the vertical distance h .

In order to obtain a clearer interpretation on Eq. (IV.37), we consider again some examples of the curved mirrors discussed in Section II :

- **Spherical mirrors.** Inserting the curvatures of the mirrors given by Eq. (II.3) into Eq. (IV.37), we obtain

$$f(h, v) = \pm \left(R - \frac{\left(1 + \frac{v^2}{c^2} \right) R^2 - \frac{v^2}{c^2} h^2}{2\sqrt{R^2 - h^2}} \right). \quad (\text{IV.38})$$

Figure 6 shows the behavior of Eq. (IV.38) for the spherical concave mirror. The intersections of the reflected rays to the principal axis can be considered as constant with respect to h at the paraxial region, and decreases with the increase of h at the outer region. However, the intersection point at a given h decreases as the speed increases. Moreover, the change of intersection points with respect to h is decreasing as the speed increases. From Figure 6, it is clear that the asymptotic behavior does not change with the change of speed.

- **Elliptic mirrors.** Inserting the curvatures of the mirrors given by Eq. (II.4) into Eq. (IV.37), we obtain

$$f(h, e, v) = \pm \left(\frac{R}{1 - e^2} + \frac{1}{2} \sqrt{R^2 - (1 - e^2)h^2} \left\{ \frac{1}{\gamma^2} - \frac{2}{1 - e^2} \frac{h^2}{R^2 - (1 - e^2)h^2} \right\} \right). \quad (\text{IV.39})$$

Figure 7 shows the behavior of Eq. (IV.39) for the elliptic concave mirror. Like the behavior of the spherical concave mirrors, the intersections of the reflected rays to the principal axis can be considered as constant with respect to h at the paraxial region, and decreases with the increase of h at the outer region. Also, the intersection point at a given h decreases as the speed increases. The change of intersection points with respect to h is again decreasing as the speed increases. Again, Figure 6 shows that the asymptotic behavior does not change with the change of speed.

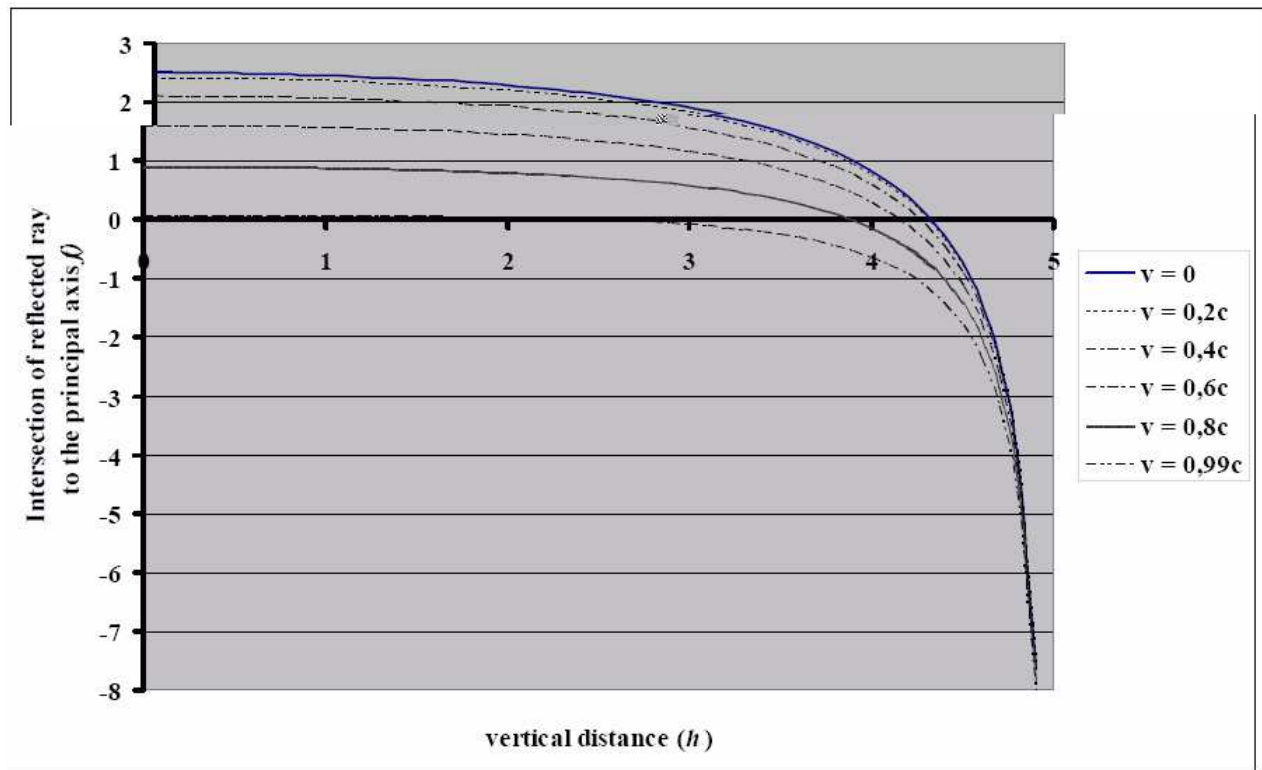


FIG. 6: A graphical representation of the spherical aberrations of spherical concave mirror with radius $R = 5$ for some moving speeds.

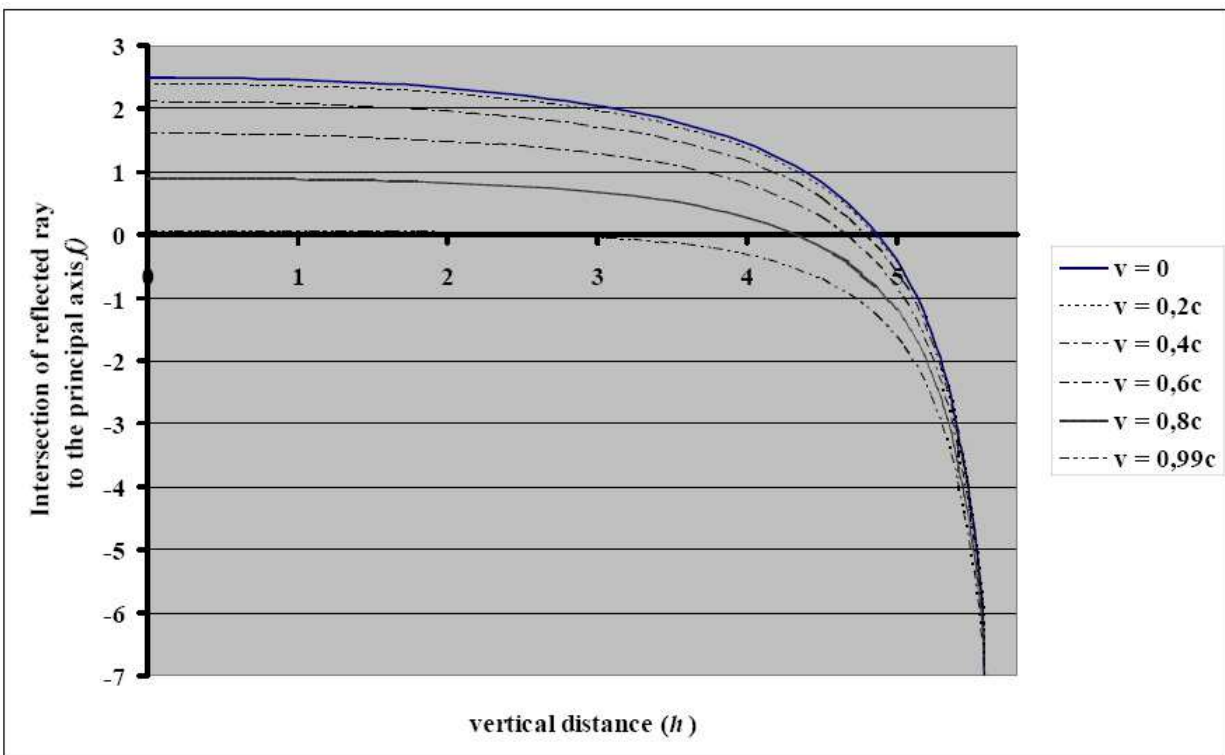


FIG. 7: A graphical representation of the spherical aberrations of elliptic concave mirror with apex $R = 5$ and eccentricity $e = 0.5$ for some moving speeds.

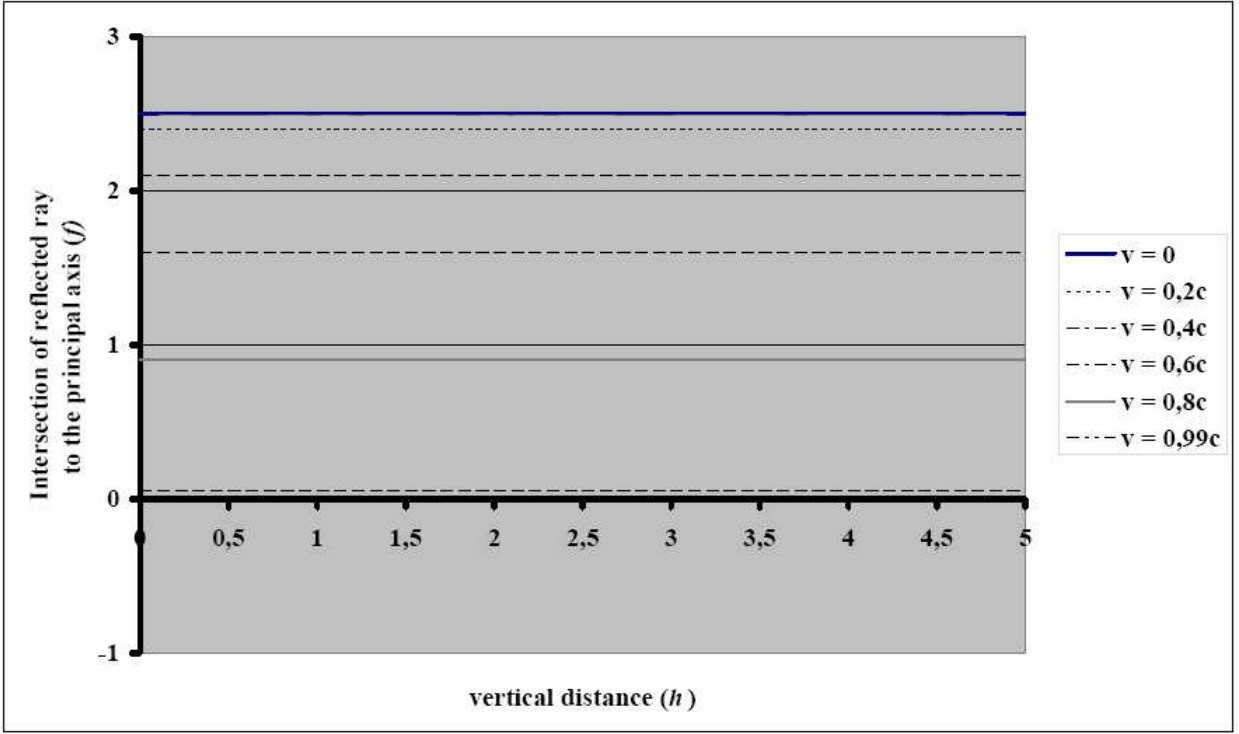


FIG. 8: A graphical representation of the spherical aberrations of parabolic concave mirror with apex $R = 5$ for some moving speeds.

- **Parabolic mirrors.** Inserting the curvatures of the mirrors given by Eq. (II.5) into Eq. (IV.37), we obtain

$$f(h, v) = \pm \frac{R}{2\gamma^2}. \quad (\text{IV.40})$$

Figure 8 shows the behavior of Eq. (IV.40) for the parabolic concave mirror. The intersections of the reflected rays to the principal axis is independent to h . Again, the intersection point decreases as the speed increases. This indicates that the parabolic mirrors do not suffer any spherical aberration in either the rest or the moving states.

- **Hyperbolic mirrors.** Inserting the curvatures of the mirrors given by Eq. (II.6) into Eq. (IV.37), we obtain

$$f(h, e, v) = \pm \left(\frac{1}{2} \sqrt{R^2 + (e^2 - 1)h^2} \left\{ \frac{1}{\gamma^2} + \frac{2}{e^2 - 1} \frac{h^2}{R^2 + (e^2 - 1)h^2} \right\} - \frac{R}{e^2 - 1} \right). \quad (\text{IV.41})$$

Figure 9 shows the behavior of Eq. (IV.41) for the hyperbolic concave mirror. The intersections of the reflected rays to the principal axis can be considered as constant with respect to h at the paraxial region, and increases with the increase of h at the outer region. The intersection point at a given h decreases as the speed increases, and the change of intersection points with respect to h is decreasing as the speed increases. Figure 9 also indicates that no asymptotic behavior is observed.

V. CONCLUSION AND FUTURE WORK

We have discussed the properties of the moving curved mirrors and compared them with the properties of the static cases. It is shown that the focal lengths of the moving mirrors are shorten by the factor $1 - \frac{v^2}{c^2}$. Consequently, all focal lengths will tend to zero as speed of the mirror systems increases up to the speed of light (if it is possible to do so). From the Gaussian formula, we may conclude that the light rays are getting harder to reach the mirror system as $v \rightarrow c$, and hence the rays are getting harder to be reflected by the surface of the mirror ($S_i \rightarrow 0$). The spherical aberrations are also affected by the movement of the mirror systems. The intersection points between the reflected rays and the principal axis decrease as the speed of the mirror systems increase, caused by the same argument that explains the decrease of the focal lengths. However, the parabolic mirrors do not

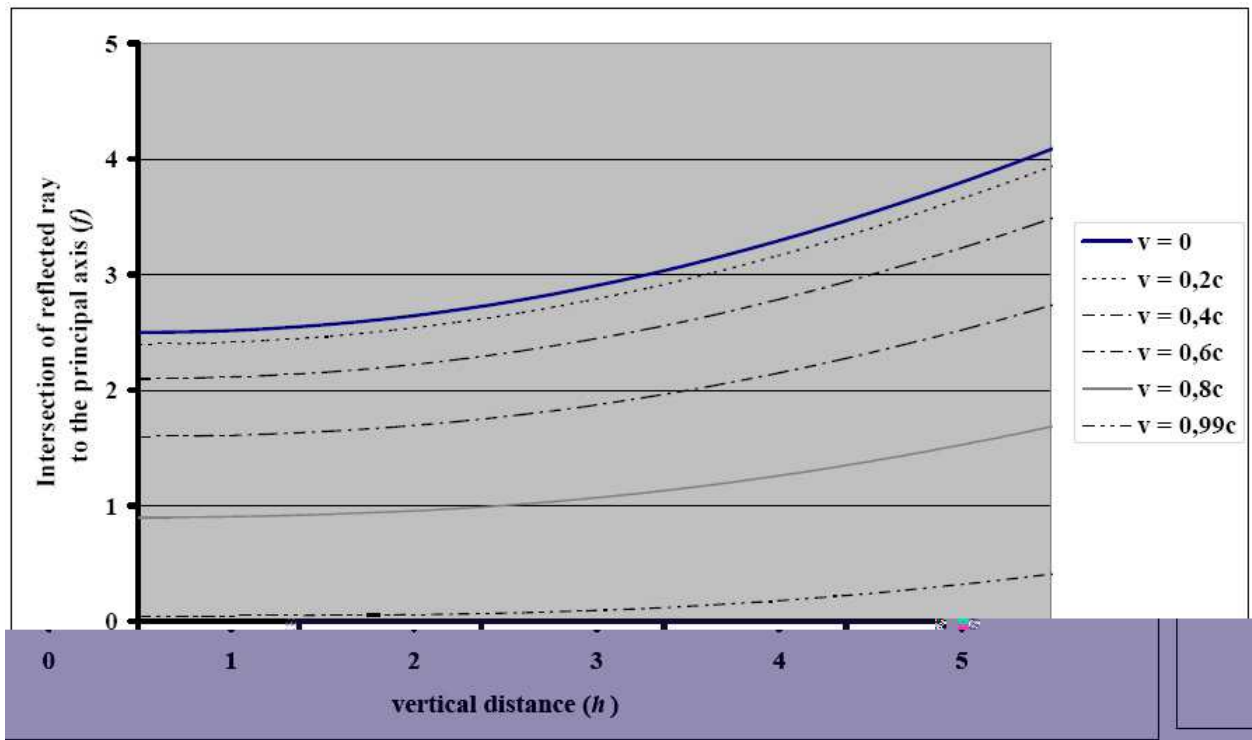


FIG. 9: A graphical representation of the spherical aberrations of hyperbolic concave mirror with apex $R = 5$ and eccentricity $e = 1.5$ for some moving speeds.

suffer any spherical aberration caused by any moving state, even though the associated focal lengths decrease with the increase of speed. For the spherical, elliptic and hyperbolic shapes of curved mirrors, the change of intersection points with respect to h decreases as the speed increases. Furthermore, the asymptotic behavior of the intersection of reflected ray to the principal axis for any shape of mirror is independent to the change of speed. The results obtained here may be useful in the constructions of curved mirrors for space vessels moving at a relativistic speed, only if we are able to build one some day.

It will be interesting to investigate whether the same techniques used in this work can be applied to the curved lens. It is well known that every lens system suffers the spherical aberration because of the change of the light speed inside the lens' media. By a logical thinking, the Gaussian formula and the spherical aberration relation must change due to the change of OPL caused by the movement of the lens system. Using the same techniques discussed here, we may discover how the speed of a lens system affects the associated focal length and spherical aberration, which can provide some new information about the behavior of moving lenses.

Acknowledgement

SHS and PCT would like to thank Dr. A. Rusli for the comments and discussions on the results at the earlier stage of this paper.

* Electronic address: sylvia@home.unpar.ac.id

† Electronic address: pctjiang@home.unpar.ac.id

¹ See, for examples : R. P. Feynman, *Lectures on Physics : Vol. I*, Addison-Wesley, pp. 26-1 - 26-8 (1963); E. Hecht, *Optics*, 4th ed., Addison-Wesley, pp. 106 - 111 (2002).

² D. S. Lemons, *Gaussian thin lens and mirror formula from Fermat's principle*, Am. J. Phys. **62**, pp. 376 (1994).

³ A. Gjurchinovski, *Reflection of light from a uniformly moving mirror*, Am. J. Phys. **72**, pp. 1316 (2004).

⁴ A. Gjurchinovski, *Einstein's mirror and Fermat's principle of least time*, Am. J. Phys. **72**, pp. 1325 (2004).

⁵ A. Einstein, *Zur Elektrodynamik bewegter Körper*, Ann. Phys. **17**, 891 (1905).

- ⁶ D. M. Watson, *Astronomy 203/403 : Astronomical Instruments and Techniques On-Line Lecture Notes*, University of Rochester (1999), <http://www.pas.rochester.edu/~dmw/ast203/Lectures/>, accessed on March 25, 2009.
- ⁷ T. Y. Baker, *Raytracing through non-spherical surfaces*, Proc. Phys. Soc. **55**, pp. 361 - 364 (1943).
- ⁸ D. Gantinel, et. al. *Determination of corneal asphericity after myopia surgery with excimer laser : a mathematical model*, Investigative Ophthalmology & Visual Science **42**, 1736 (2001).
- ⁹ E. Hecht, *Optics*, 4th ed., Addison-Wesley, p. 226 (2002).